



CHORUS

This is the accepted manuscript made available via CHORUS. The article has been published as:

Charge Resonance Enhanced Ionization of CO₂ Probed by Laser Coulomb Explosion Imaging

Irina Bocharova, Reza Karimi, Emmanuel F. Penka, Jean-Paul Brichta, Philippe Lassonde, Xiquan Fu, Jean-Claude Kieffer, André D. Bandrauk, Igor Litvinyuk, Joseph Sanderson, and François Légaré

Phys. Rev. Lett. **107**, 063201 — Published 2 August 2011

DOI: [10.1103/PhysRevLett.107.063201](https://doi.org/10.1103/PhysRevLett.107.063201)

Charge resonance enhanced ionization of CO₂ probed by laser Coulomb explosion imaging

Irina Bocharova¹, Reza Karimi², Emmanuel F. Penke³, Jean-Paul Brichta⁴, Philippe Lassonde⁵,
Xiquan Fu⁷, Jean-Claude Kieffer⁵, André D. Bandrauk³, Igor Litvinyuk⁶, Joseph Sanderson²,
François Légaré⁵

¹ J.R. Macdonald Laboratory, Physics Department, Kansas State University, Manhattan, KS
66503

² Department of Physics and Astronomy University of Waterloo, Waterloo, 200 University
Avenue West, ON, Canada N2L 3G1

³ Département de Chimie, Université de Sherbrooke, Sherbrooke, Qc Canada J1K 2R1

⁴ Department of Physics, University of Ottawa, 150 Louis-Pasteur, Ottawa, On Canada K1N6N5

⁵ Institut National de la Recherche Scientifique, Centre Énergie Matériaux Télécommunications,
Varenes, Qc Canada J3X1S2

⁶ Centre for Quantum Dynamics, Griffith University, Nathan, Queensland 4111, Australia

⁷ School of Computer and Communication, Hunan Changsha 410082, China

The process by which a molecule in an intense femtosecond laser field ionizes more efficiently as its bond length increases towards a critical distance R_c is known as charge resonance enhanced ionization (CREI). For the first time we make a series of measurements of this process for a polyatomic molecule, CO_2 , by varying pulse duration, from 7fs to 200fs in order to identify, the charge states and timescale involved. We reconstruct the geometry at the moment of explosion and obtained the critical geometry ($\langle R_{\text{CO}} \rangle \approx 2.1 \text{ \AA}$ and $\langle \theta_{\text{OCO}} \rangle \approx 163^\circ$, compared to equilibrium values of $\langle R_{\text{CO}} \rangle \approx 1.16 \text{ \AA}$ and $\langle \theta_{\text{OCO}} \rangle \approx 172^\circ$). We find that for the 4+ and higher charge states, 100fs, is the critical timescale. The CO_2^{3+} molecule however appears always to begin dissociation from closer than 1.7 \AA indicating that dynamics on charge states lower than 3+ are not sufficient to initiate CREI. Finally, we make the first quantum numerical simulations of ionization rate for a polyatomic molecule in an intense field and identify the electronic states ($3\sigma_u$ and $5\sigma_g$) responsible for CREI in our experimental observations of CO_2 .

Ultrafast molecular imaging techniques with intense infrared femtosecond laser pulses are based on converting long wavelength photons into short wavelength particles via the process of ionization: XUV photons for orbital tomography [1], electrons for laser induced electron self-diffraction [2,3], and ions for time-resolved Coulomb Explosion Imaging (CEI) [4-6]. It is therefore critical to understand the different mechanisms behind high intensity molecular ionization.

In the case of CEI, experiments with diatomics have shown that the molecular bond stretches towards a critical internuclear distance (R_C) where the ionization rate is greatly enhanced [7,8]. This also explains the explosion of clusters creating highly charged states [9]. This process called CREI is well understood for diatomic molecules, such as H_2^+/D_2^+ , in terms of charge resonance (CR) states (σ_g and σ_u) that are strongly coupled by the laser field at large internuclear distance [10-12]. At such distances, the energy difference between the two CR states approaches the photon energy, giving rise to electron localization by creating a coherent superposition of opposite parity states [13] followed by enhanced ionization. For triatomic molecules, the experimental appearance of a critical geometry has not been elucidated in terms of CREI and its mechanism remains a matter of interest.

CO_2 has been the subject of experiments using both uncorrelated and correlated fragment detection techniques [14-16]. All those studies used pulses of 50 fs and longer and have attempted to understand the mechanism of dissociative ionization. Two consistent parts of the picture which have emerged are that the bond lengths determined from a Coulombic inversion appear to be stretched between 2 and 2.5 times the equilibrium distance to a critical distance (R_C) and the bond angle is less than 180 degrees. Experimental results for CO_2 have been compared to classical calculations [15,16] adapted from the over the barrier model developed by Posthumus et

al. [17]. This simple approach predicts a value for R_C but for bonds stretched considerably more than indicated by experimental observations. Numerical simulations of nuclear motion on field dressed molecular potentials of CO_2^{2+} have revealed bending and symmetric stretching on a time scale of ~ 100 fs [18]. These vibrational dynamics cannot explain the observation of a R_C when CO_2 is ionized to high charge states ($> 3+$). To our knowledge, no experimental work has successfully tracked the dynamics on either the doubly or higher charged states and no theoretical work has modeled the mechanism for CREI in triatomic molecules including CO_2 .

It has been demonstrated for diatomics that by using few-cycle pulses, CREI can be suppressed since the molecular ion does not have sufficient time to reach R_C within the duration of the pulse [19]. Therefore, varying the pulse duration from the few-cycle to the multi-cycle regime is a valid approach to follow the appearance of CREI and investigate its molecular origin. In this letter, we use 3D-ion-momentum coincidence measurements of the three-body dissociative ionization of CO_2 to CO_2^{n+} ($n=3$ to 6) with linearly polarized 800 nm laser pulses to make the first systematic study of the dependence of dissociative multiple ionization dynamics on laser pulse duration for any polyatomic molecule. We achieve this by varying the pulse duration from 7 fs up to 200 fs to find the onset of CREI. We then perform nonlinear nonperturbative time-dependent density functional theory (TDDFT) calculations to attempt to identify the CR states and thus the underlying mechanism for CREI in CO_2 .

The experiments were performed at the Advanced Laser Light Source using the multi-kHz Titanium-Sapphire (Ti-Sa) laser system (KMLabs). Few-cycle pulses (7 fs) are obtained using nonlinear propagation in a hollow core fiber filled with Ar and by dispersion compensation using chirped mirrors. To achieve longer pulse duration, the fiber was evacuated. Using an acousto-optic programmable dispersive filter located in the stretcher of the Ti-Sa amplifier, we

applied second order dispersion ($\Phi^{(2)}(\text{fs}^2)$) to achieve the desired pulse duration. The laser pulses are focused by a parabolic mirror ($f = 10 \text{ cm}$) on a well-collimated supersonic jet of CO_2 inside a uniform-electric-field ion imaging spectrometer. The fragments are detected and their full 3D momenta are determined using a time- and position-sensitive delay-line anode detector at the end of the spectrometer (RoentDek Handels GmbH). We measured the atomic fragment ions in triple coincidence: O^{k+} , C^{q+} and O^{l+} ions are identified as the result of the fragmentation of a single molecule only if their total momentum is close to zero ($< 5 \times 10^{-23} \text{ kg} \times \text{m/s}$).

For 7 fs, we observe that a much higher intensity is required to produce high charge states such as C^{2+} and O^{2+} . Figure 1(a) compares the time-of-flight mass spectra for 7 fs $I=2 \times 10^{15} \text{ W/cm}^2$ and 200 fs $I=2 \times 10^{14} \text{ W/cm}^2$ giving the same ratio of C^{2+}/C^+ ion yields. This observation confirms that ionization of CO_2 to high charge states is much easier for multi-cycle pulses, i.e. CREI is suppressed with few-cycle pulses [19]. In addition, for 200 fs duration, the forward and backward O^{2+} peaks are quite narrow and the signal drops to zero between them, whereas for the 7 fs pulse the peaks are wide with continuous signal in between. For a long pulse, the molecules are preferentially ionized along the laser polarization axis (which here is along the spectrometer time-of-flight axis). For 7 fs, in contrast, some ions are produced with angles close to 90 degrees with respect to the polarization axis. This is confirmed in figure 1(b) where the angular distributions of O^{2+} are plotted (7 fs $I=2 \times 10^{15} \text{ W/cm}^2$, 35 fs $I=8 \times 10^{14} \text{ W/cm}^2$, 200 fs $I=2 \times 10^{14} \text{ W/cm}^2$). Although dynamic alignment may play a role above 35 fs, a dramatic broadening of fragment angular distributions such as the one observed for 7 fs has previously been reported for the Coulomb explosion of D_2 and is explained by the suppression of CREI [19].

We now discuss the results obtained from triple coincidence measurements. Figure 2(a,b) shows the total kinetic energy release (KER) for the (1,1,1 – $\text{O}^+ + \text{C}^+ + \text{O}^+$) and the (2,2,2 –

$O^{2+}+C^{2+}+O^{2+}$) channels measured as a function of pulse duration. It should be noted that no intensity dependence was found for the peak position of the kinetic energy distributions (at fixed pulse duration). For the (2,2,2), there is a clear trend of increasing KER with decreasing pulse duration. From 200 fs to 35fs, the KER increases from around 50% to 60% of the expected Coulombic value. For 7 fs pulses, there is a significant increase of KER up to 90% of the Coulombic value. If we relate the KER to the bond lengths at which the final charge state is populated, it is apparent that the molecule is being ionized at progressively longer bond lengths as the pulse duration increases, and reaches R_C at a pulse duration near to 100 fs. For diatomics, the observation of R_C has been explained by the presence of CREI [11-13].

By contrast, the (1,1,1) channel exhibits a quite different behavior with KER at around 70-75% of the Coulombic value independent of the pulse duration. This independence of pulse duration, never reported before, is summarized in figure 2(c). The observation is consistent with dissociation from a non Coulombic potential, one in which bond length does not map onto the total KER. The ground state of CO_2^{3+} exhibits this kind of behavior for $R < 1.7\text{\AA}$ where the potential is weakly attractive; as can be seen in figure 5 of reference [18]. When the dissociating wave packet reaches $R_{CO}=1.7\text{\AA}$ it then experiences full Coulombic repulsion releasing approximately 70% of the energy expected from equilibrium plus energy accumulated on lower dissociative states. The results indicate that even with few-cycle pulses, it is not possible to retrieve the molecular structure of CO_2 using CO_2^{3+} as the final charge state. However, by looking at the KE spectra of C^+ and O^+ , we can infer dissociation dynamics on lower charge states. Figure 2(d,e) presents the C^+ and O^+ KE spectra as a function of pulse duration. We observe that as the pulse duration increases, the C^+ KE spectrum broadens towards high energy, and correlates with an opposite behavior in O^+ which moves to lower KE. This is a significant

observation as it indicates bending dynamics on lower charge states. Our observations are the first time dependent confirmation of the predictions of Sato et al. [18] who have modeled dissociation dynamics on the light dressed states of CO_2^{2+} , without considering the ionization step to CO_2^{3+} , and predicted bending in association with symmetric stretching to between 1.4 and 1.75 Å bond length on time scale of ~ 100 fs.

Figure 2(c) also presents the KER as a function of pulse duration for higher final charge states. *We observe that the KER becomes significantly dependent on the pulse duration but only for the 4+ and higher charge states.* With 7 fs duration and for final charge states higher than 3+, the KER is close to the value expected for Coulomb explosion from the CO_2 equilibrium geometry. For longer pulse duration, the total KER decreases and it becomes almost independent of pulse duration (>100 fs) in a similar fashion to the pulse duration dependence of KER from D_2 in a pulse longer than ~ 40 fs [19]. For D_2 the KER from Coulomb explosion becomes independent of pulse duration once the D_2^+ molecular ion stretches to R_C , where CREI occurs [11-13]. In figure 2(c), the variation in %CE (Coulomb Energy) between channels, for long pulse duration experiments, at first glance appears to indicate a variation in R_C with final charge state (assuming a Coulombic $1/R$ inversion, 50% of CE implies $R_C=2R_{\text{Equilibrium}}$). However, to conclude this would be incorrect as this variation is mainly attributable to the contribution to the final channel KER from the dissociation of CO_2^{3+} (which does not change with pulse duration). In the case of (1,1,2), this is a large fraction of the final energy but becomes progressively less important for the 5+ (1,2,2) and the 6+ (2,2,2) charge states. In fact, it is quite straightforward to show that the actual value of R_C for the (1,1,1) to (1,1,2) step is between 1.85 and 2 Å [20]. This indicates that significant dissociative dynamics must be occurring on the 3+ charge state, in order to stretch from 1.7 Å to 2 Å. By performing full coincidence momentum measurements, it is

possible to retrieve the molecular structure [4]. We have chosen the highest observed charge state 6+ (2,2,2) to perform this retrieval. A simplex algorithm is used to iteratively optimize the agreement between the measured momenta and the asymptotic momenta generated by a simulation of the Coulomb explosion of the molecule in the 6+ state. Recently, this algorithm has been refined and presented in detail [21]. Figure 3(a) presents the retrieved molecular structure ($\langle R_{CO} \rangle \approx 1.3 \text{ \AA}$ and $\langle \theta_{OCO} \rangle \approx 168^\circ$) for 7 fs pulses which is very close to the equilibrium geometry ($\langle R_{CO} \rangle = 1.16 \text{ \AA}$ and $\langle \theta_{OCO} \rangle \approx 172^\circ$ [22]). Figure 3(b) summarizes our experimental observations; the molecular structure of CO₂ remains almost unchanged ($\langle R_{CO} \rangle \approx 2.1 \text{ \AA}$ and $\langle \theta_{OCO} \rangle \approx 163^\circ$) for pulse duration longer than 100 fs.

Molecular structures presented in figure 3 reveal that CO₂ undergoes ultrafast symmetric stretching in the presence of the laser field. Figure 2(c) indicates that this symmetric stretching cannot be explained by nuclear dynamics on the CO₂²⁺ potential energy surface since the KER from CO₂³⁺ is almost independent of pulse duration. As mentioned previously, Sato *et al.* calculated that about 100 fs is required for symmetric bond stretching between 1.4 and 1.75 Å to occur on light dressed CO₂²⁺ [18], which is significantly shorter than the measured R_C . This is confirmed in figure 3 where we show that R_{CO} is already stretched to $\sim 1.75 \text{ \AA}$ with pulse duration of 35 fs. *The strong dependence of KER on pulse duration is only observed when the 4+ charge state is reached, revealing significant dissociative dynamics on the 3+ and higher charge states, with 3+ providing the first step of CREI.* To elucidate this mechanism, we have calculated the ionization rate and the electronic structure of CO₂³⁺ as a function of R_{CO} assuming a symmetric linear geometry which is a valid approximation based on the structure presented in figure 3.

We have performed nonlinear nonperturbative TDDFT using the SAOP (statistical average of orbital potential) local density potential to calculate the ionization rate [23] of CO_2^{3+} as a function of R_{CO} with the following parameters: $I=8\times 10^{14}$ W/cm², $\lambda = 800$ nm, $\tau = 6$ optical cycles. Triple-zeta (TZ2P) Slater-type orbital (STO) basis set have been used for all atoms. A symmetric linear geometry for CO_2^{3+} was assumed. For each R_{CO} , two calculations were performed; the molecular axis is either parallel or perpendicular to the polarization axis. The ionization rate per optical cycle is presented in figure 4(a). The ionization rate when CO_2^{3+} is perpendicular to the laser polarization axis remains constant for R_{CO} longer than ~ 1.7 Å while it continues to increase when the molecule is parallel. At the largest R_{CO} where calculations can be performed, near 1.9 Å, the ionization rate is ~ 5 times larger when CO_2^{3+} is parallel to the polarization axis. Therefore, we conclude that as CO_2^{3+} is symmetrically breaking apart within the laser field, the intensity required to reach high charge states decreases due to increased ionization rate and the distribution of high charge fragments such as O^{2+} becomes highly anisotropic, and peaked along the polarization axis. This explains the experimental results presented in figure 1.

From the nonlinear nonperturbative TDDFT calculations, we can identify the probability of ionization as a function of the molecular orbital. We observe that the ionization probability is mostly coming from the $3\sigma_u$ orbital when CO_2^{3+} is parallel to the polarization, while it comes from the $1\pi_u$ orbital for the perpendicular case. To understand these results, time-independent DFT calculations [24] were performed to characterize the electronic structure of CO_2^{3+} as a function of R_{CO} . At the equilibrium of CO_2 , we find for the 3+ charge state that the HOMO in $D_{\infty h}$ is an anti-bonding type, $1\pi_g$, formed of π lobes lying perpendicular to the internuclear axis and located on the oxygen atoms, while the HOMO-1 is $3\sigma_u$, and the HOMO-2 is $1\pi_u$. At $R\approx 2$ Å,

they become almost degenerate. The energy gaps and the transition moments for parallel transitions; $3\sigma_u \rightarrow 5\sigma_g$ (Σ), $1\pi_u \rightarrow 1\pi_g$ (Π_a), and $1\pi_g \rightarrow 2\pi_u$ (Π_b), are presented in figure 4(b,c).

To explain CREI in term of strongly coupled CR states, both the Σ ($3\sigma_u \rightarrow 5\sigma_g$) and the Π_a ($1\pi_u \rightarrow 1\pi_g$) parallel transitions can result in charge localization. The ionization rate is however much higher from the $3\sigma_u$ as mentioned previously. Charge localization from the Π_a transition results in a p shape orbital with its main axis perpendicular to the laser polarization, from which the ionization rate is suppressed [25]. Finally, the Π_b transition is much less important because at large R_{CO} , the $2\pi_u$ becomes localized on the carbon as a 2p atomic orbital in the center of the molecule while the electronic density of the $1\pi_g$ orbital is located on the oxygen atoms in a 2p atomic orbital separated by $2R_{CO}$. The resulting transition moment and radiative coupling vanishes with increasing R_{CO} .

In conclusion, we have made the first clear systematic measurements and provided interpretation of the effect of laser pulse duration on dissociative ionization to high charge states for a polyatomic molecule, CO_2 . By changing the pulse duration, we have been able to definitively measure the molecular geometry where CREI occurs ($\langle R_{CO} \rangle \approx 2.1 \text{ \AA}$ and $\langle \theta_{OCO} \rangle \approx 163^\circ$). The experimental results clearly indicate the importance of dissociation dynamics on the CO_2^{3+} charge state leading to structural deformation observed in the higher charge states. As the CO_2^{3+} breaks apart, the numerical simulations clearly show that the ionization rate increases rapidly when the molecule is aligned along the laser polarization axis because of strongly coupled CR states ($3\sigma_u \rightarrow 5\sigma_g$). This requires that enough time is given to CO_2^{3+} and subsequent charge states to stretch up to the critical distance of $R_{CO} \sim 2 \text{ \AA}$, a condition satisfied with laser pulse duration equal to or longer than 100 fs.

Acknowledgments

The authors acknowledge the support of the CFI, CIPI, NSERC, CRC and FQRNT. IB and IL acknowledge support of US Department of Energy.

References

- [1] J. Itatani, J. Levesque, D. Zeidler, H. Niikura, H. Pépin, J-C. Kieffer, P. B. Corkum, and D. M. Villeneuve, *Nature* **432**, 867 (2005).
- [2] T. Zuo, A. D. Bandrauk, and P. B. Corkum, *Chem. Phys. Lett.* **259**, 313 (1996).
- [3] M. Meckel, D. Comtois, D. Zeidler, A. Staudte, D. Pavičić, H. C. Bandulet, H. Pépin, J-C. Kieffer, R. Dörner, D. M. Villeneuve, and P. B. Corkum, *Science* **320**, 1478 (2008).
- [4] F. Légaré, K. F. Lee, I. V. Litvinyuk, P. W. Dooley, A. D. Bandrauk, D. M. Villeneuve, and P. B. Corkum, *Phys. Rev. A* **72**, 052717 (2005).
- [5] A. Hishikawa, A. Matsuda, M. Fushitani, and E. J. Takahashi, *Phys. Rev. Lett.* **99**, 258302 (2007).
- [6] C. Cornaggia, *Las. Phys.* **19**, 1660 (2009).
- [7] K. Codling and L. J. Frasinski, *J. Phys. B: At. Mol. Opt. Phys.* **26**, 783 (1993).
- [8] M. Schmidt, D. Normand, and C. Cornaggia, *Phys. Rev. A* **50**, 5037 (1994).
- [9] C. Siedschlag and J. M. Rost, *Phys. Rev. A* **67**, 013404 (2003).
- [10] T. Seideman, M. Yu. Ivanov, and P. B. Corkum, *Phys. Rev. Lett.* **75**, 2819 (1995).
- [11] T. Zuo and A. D. Bandrauk, *Phys. Rev. A* **52**, R2511 (1995).
- [12] S. Chelkowski and A. D. Bandrauk, *J. Phys. B* **28**, L723 (1995).

- [13] A. Staudte, D. Pavičić, S. Chelkowski, D. Zeidler, M. Meckel, H. Niikura, M. Schöffler, S. Schössler, B. Ulrich, P. P. Rajeev, Th. Weber, T. Jahnke, D. M. Villeneuve, A. D. Bandrauk, C. L. Coker, P. B. Corkum, and R. Dörner, *Phys. Rev. Lett.* **98**, 073003 (2007).
- [14] L. J. Frasinski, P. A. Hatherly, K. Codling, M. Larsson, A. Persson, and C. G. Wahlstrom, *J. Phys. B: At. Mol. Opt. Phys.* **27** L109 (1994).
- [15] A. Hishikawa, A. Iwamae, and K. Yamanouchi, *Phys. Rev. Lett.* **83**, 1127 (1999).
- [16] J. P. Brichta, S. J. Walker, R. Helsten, and J. H. Sanderson, *J. Phys. B: At. Mol. Opt. Phys.* **40**, 117 (2007).
- [17] J. H. Posthumus, L. J. Frasinski, A. J. Giles, and K. Codling, *J. Phys. B: At. Mol. Opt. Phys.* **28**, L349 (1995).
- [18] Y. Sato, H. Kono, S. Koseki, and Y. Fujimura, *J. Am. Chem. Soc.* **125**, 8019 (2003).
- [19] F. Légaré, I. V. Litvinyuk, P. W. Dooley, F. Quéré, A. D. Bandrauk, D. M. Villeneuve, and P. B. Corkum, *Phys. Rev. Lett.* **91**, 093002 (2003).
- [20] S. V. Menon, J. P. Nibarger, and G. N. Gibson, *J. Phys. B: At. Mol. Opt. Phys.* **35**, 2961 (2002).
- [21] J-P. Brichta, A. N. Seaman, and J. H. Sanderson, *Comp. Phys. Comm.* **180**, 197 (2009).
- [22] B. Siegmann, U. Werner, H. O. Lutz, and R. Mann, *J. Phys. B: At. Mol. Opt. Phys.* **35**, 3755 (2002).
- [23] O. V. Gritsenko, P. R. T. Schipper, and E. J. Baerends, *Chem. Phys. Lett.* **302**, 199 (1999).
- [24] E. P. Fowe and A. D. Bandrauk, *Phys. Rev. A* **81**, 023411 (2010).
- [25] G. Lagmago Kamta and A. D. Bandrauk, *Phys. Rev. A* **75**, 041401(R) (2007).

Figure captions

Figure 1: (a) Mass/q spectra obtained for two experimental conditions; 7 fs $I = 2 \times 10^{15}$ W/cm² and 200 fs $I = 2 \times 10^{14}$ W/cm². (b) Angular distribution of O²⁺ fragments relative to the laser polarization direction as a function of laser pulse duration; 7 fs $I = 2 \times 10^{15}$ W/cm², 35 fs $I = 8 \times 10^{14}$ W/cm², and 200 fs $I = 2 \times 10^{14}$ W/cm².

Figure 2: Spectra of total KER (kinetic energy released) as a function of laser pulse duration for (a) the (1,1,1) and (b) the (2,2,2) final charge state. (c) Ratio of kinetic energy released to energy expected from Coulomb Explosion at the equilibrium of CO₂ (CE) as a function of the final charge states and pulse duration. Spectra of (d) C⁺ and (e) O⁺ kinetic energy released as a function of pulse duration for the (1,1,1) final charge state. For (a,b,d,e) the legend is: 7 fs – square, 35 fs – circle, 60 fs – triangle up, 100 fs – triangle down, 200 fs – diamond. For the (1,1,1) measurements, the laser intensities (W/cm²) are: 7 and 35 fs; 5×10^{14} , 60, 100 and 200 fs; 3×10^{14} . For the measurements where the final charge state is $\geq 4+$, the laser intensities (W/cm²) are: 7 fs; 2×10^{15} , 35 fs; 8×10^{14} , 60 fs; 5×10^{14} , 100 fs; 4×10^{14} ; 200 fs; 3×10^{14} .

Figure 3 (a) Retrieved molecular structure for 7 fs pulse duration using the (2,2,2) final charge states. (b) Average CO bond distance and bend angle retrieved as a function of pulse duration.

Figure 4. Results of numerical simulations. (a) Ionization rate per optical cycle as a function of R_{CO} for CO₂³⁺. (b,c) Energy gaps (eV) and transition moments (a.u.) for the parallel transitions in CO₂³⁺.

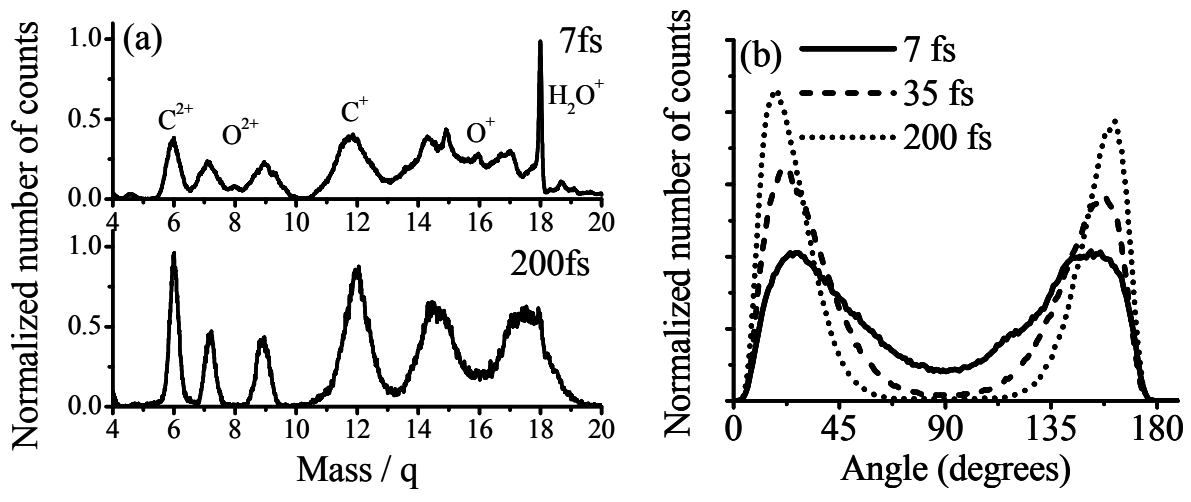


Figure 1

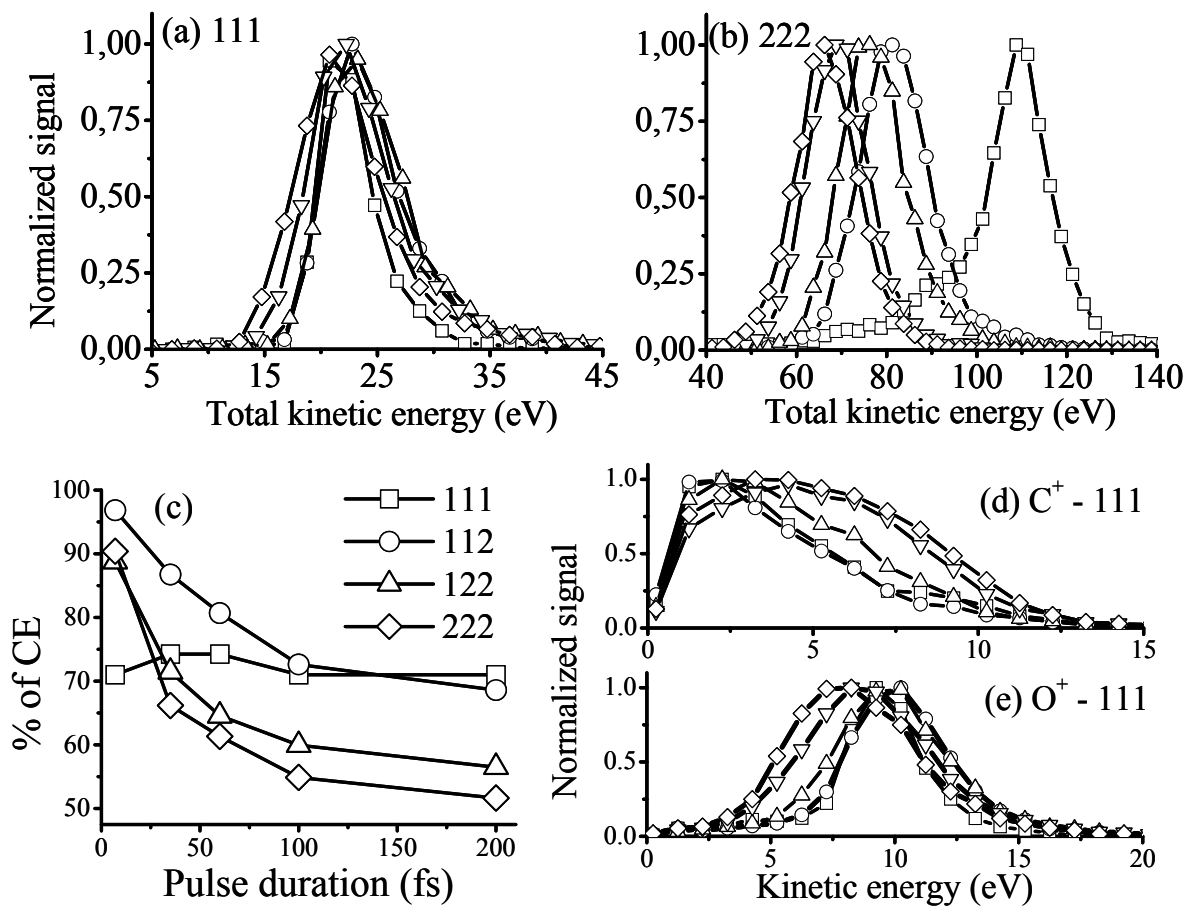


Figure 2

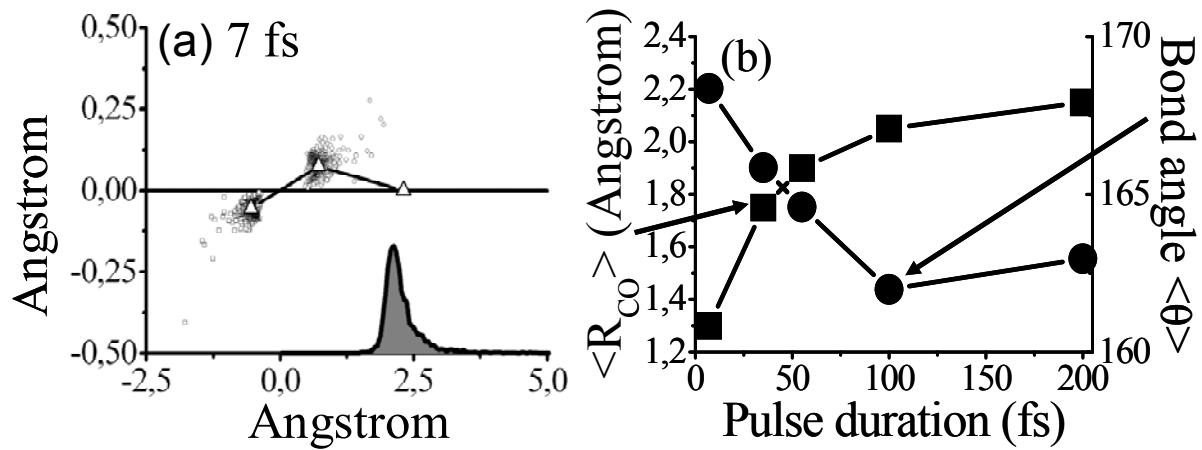


Figure 3

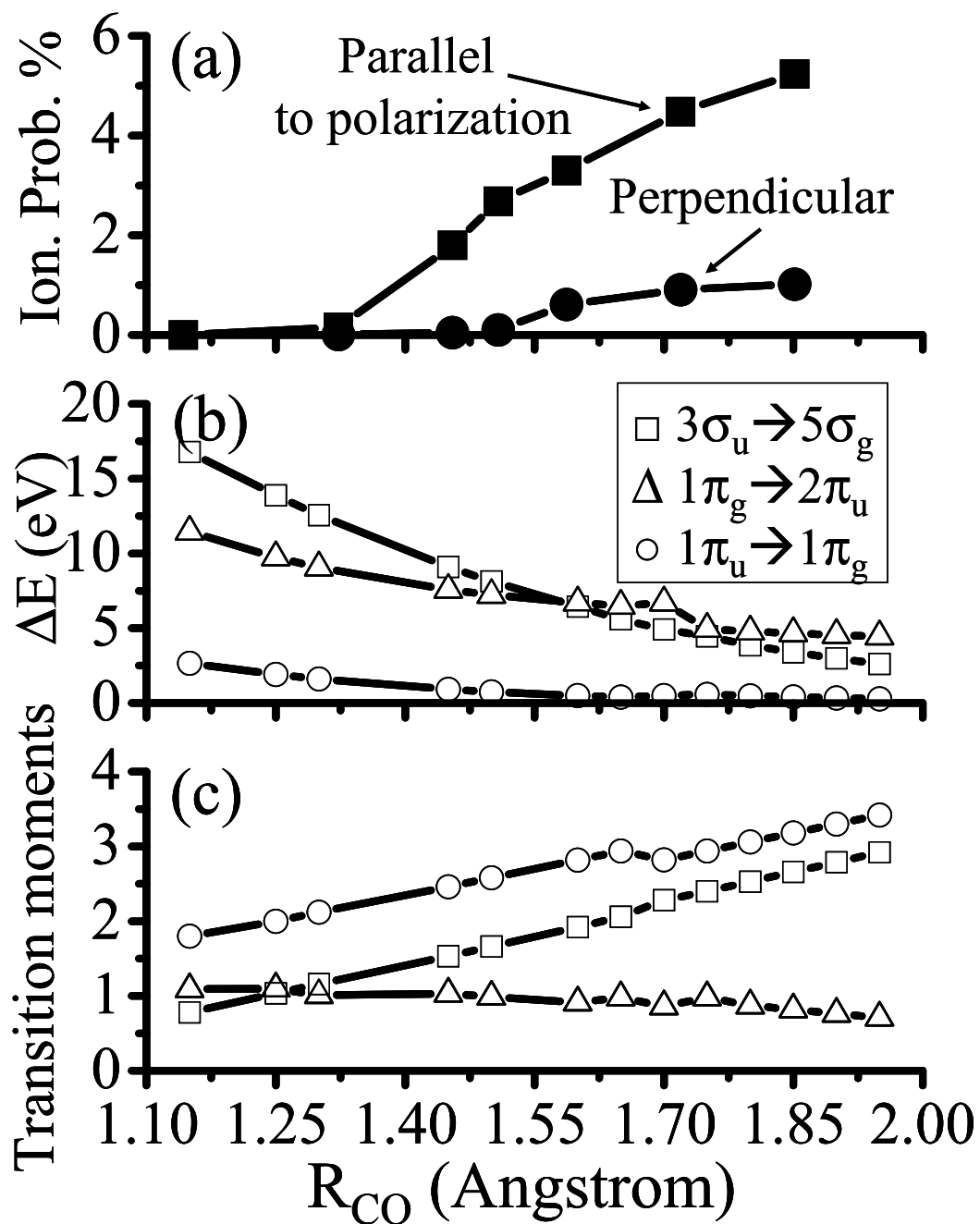


Figure 4